

Relation between susceptibility and Knight shift in $\text{La}_2\text{NiO}_{4.17}$ and K_2NiF_4 by ^{61}Ni NMR

J. J. van der Klink¹ and H. B. Brom²¹*IPN-SB, EPFL, station 3, CH-1015 Lausanne, Switzerland*²*Kamerlingh Onnes Laboratory, Leiden University, P.O. Box 9504, 2300 RA Leiden, The Netherlands*

(Received 16 September 2009; revised manuscript received 15 January 2010; published 17 March 2010)

The NiO_4 plaquettes in $\text{La}_2\text{NiO}_{4.17}$, a cousin of the hole-doped high-temperature superconductor $\text{La}_{2-x}\text{Sr}_x\text{CuO}_4$, have been studied by ^{61}Ni NMR in 14 T in a single crystal enriched in ^{61}Ni . Doped and undoped plaquettes are discriminated by the shift of the NMR resonance, leading to a small line splitting, which hardly depends on temperature or susceptibility. The smallness of the effect is additional evidence for the location of the holes as deduced by Schüßler-Langenhene *et al.* [Phys. Rev. Lett. **95**, 156402 (2005)]. The increase in linewidth with decreasing temperature shows a local-field redistribution, consistent with the formation of charge-density waves or stripes. For comparison, we studied, in particular, the grandmother of all planar antiferromagnets K_2NiF_4 in the paramagnetic state using natural abundant ^{61}Ni . The hyperfine fields in both two-dimensional compounds appear to be remarkably small, which is well explained by super(transferred) hyperfine interaction. In K_2NiF_4 , the temperature dependence of the susceptibility and the Knight shift cannot be brought onto a simple scaling curve. This unique feature is ascribed to a different sensitivity for correlations of these two parameters.

DOI: [10.1103/PhysRevB.81.094419](https://doi.org/10.1103/PhysRevB.81.094419)

PACS number(s): 76.60.-k, 74.72.-h, 75.30.Ds, 75.40.Gb

I. INTRODUCTION

In a seminal paper, Zhang and Rice showed the validity of a single-band effective Hubbard Hamiltonian starting from a two-band model for the superconducting copper oxides.¹ Although the holes created by doping reside primarily on the oxygen sites, Cu-O hybridization strongly binds this hole to the central $\text{Cu}^{2+}3d^9$ ion of the square-planar CuO_4 plaquette to form a singlet, nowadays called “Zhang-Rice” singlet. This singlet then moves through the lattice of Cu^{2+} ions in a similar way as a hole in the single-band Hamiltonian.

Around the same time, Zaanen and Gunnarsson used a three-band Hubbard model to describe the Cu-O perovskite plane, including the oxygen $2p$ and Cu $3d_{x^2-y^2}$ states and argued that charge and spins in a two-dimensional (2D) electronic system with strong correlations could form charge- and spin-density waves with spins being maximal where the charges are absent.² This striped structure appeared also in other theoretical approaches³ but had to wait until 1995 for a convincing experimental verification by elastic neutron scattering in Sr/Nd-doped La_2CuO_4 and oxygen-doped La_2NiO_4 .⁴

Apart from the formation of striped structures, doped cuprates and nickelates have other similarities but also obvious differences. While delocalized holes in the cuprates finally lead to superconductivity, holes in the nickelates experience strong self-localization, and for doping levels less than one the nickelates are insulators. Still, on the length scale of a lattice constant, the dressed holes or polarons can be seen as nonclassical objects.⁵ Like in the doped cuprates, the holes in the nickelates are mainly located on the in-plane oxygen, as shown for $\text{La}_{1.8}\text{Sr}_{0.2}\text{NiO}_4$ by resonant soft x-ray diffraction.⁶ Here “undoped Ni^{2+} ” and “doped Ni^{3+} ” ions correspond to objects with 8.2, respectively, 7.9 $3d$ electrons, the latter accompanied by an antiferromagnetically coupled hole in the oxygen ligand orbital of x^2-y^2 symmetry.⁶ Since in both cases, the Ni ion is close to a $3d^8$ configuration with spin

$S=1$, the doped plaquette has a net spin of 1/2 instead of zero spin in the cuprates.

The present paper investigates to what extent ^{61}Ni NMR can give additional information about the difference between a $3d^7$ Ni^{3+} ion and a doped plaquette with a (close to) $3d^8$ ion at its center. Although the NMR technique for $\text{La}_2\text{NiO}_{4.17}$ is severely hindered by signal wipe out due to magnetic fluctuations below 70 K and by oxygen disordering above 250 K,^{7,8} we will argue that even in this temperature (T) range, two types of plaquettes can be distinguished on the NMR time scale, and that the results are independent evidence for the dressed $3d^8$ picture for the doped plaquettes proposed in Ref. 6. Furthermore, we find a T dependence of the linewidth that is consistent with the formation of charge-density waves or stripes, as seen in Sr-doped La_2NiO_4 with a similar doping concentration.⁹ To put our results in perspective, we have a closer look into the paramagnetic phase of three- and two-dimensional (3D and 2D) antiferromagnets and, in particular, study the relation between Knight shift K and susceptibility χ in the paramagnetic state of the grandmother of all square-planar antiferromagnets K_2NiF_4 —one of the first studies of this kind. Since hardly any ^{61}Ni NMR work in nonmetallic paramagnetic systems has been published, we give some background considerations for convenience in the Appendix.

II. EXPERIMENTAL

Several groups have investigated the location of the excess oxygen site, possible staging and uniformity in $\text{La}_2\text{NiO}_{4+\delta}$ as a function of δ with slightly different results.^{10–14} In $\text{La}_2\text{NiO}_{4.18}$, the structure is (almost) tetragonal with $2c/(a+b)=2.32$ (Ref. 10) while the excess oxygen is located at interstitial sites equivalent to (0.183, 0.183, 0.217).¹³

The studied single crystal ($10 \times 3 \times 1$ mm), enriched to 20% with ^{61}Ni , was grown in a mirror oven in a similar way as the unenriched samples measured before and had similar

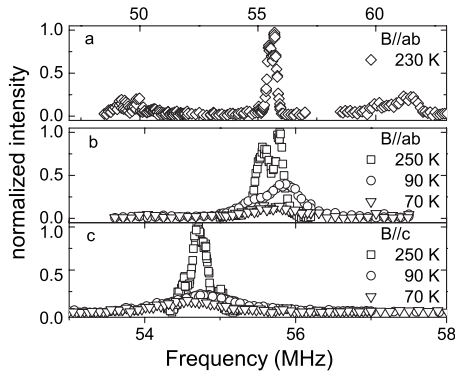


FIG. 1. NMR spectra for $\text{La}_2\text{NiO}_{4.17}$ (a) broad frequency sweep (top axis) for $B||ab$ at 230 K showing the quadrupole splitting. (b) and (c) Spectra for $B||ab$, respectively, $B||c$ at three different temperatures (bottom axis). If field conventions are followed, the spectrum has to be plotted in reverse order.

^{139}La NQR spectra.^{7,8} X-ray diffraction at room temperature resulted in a sharp line pattern. Refinement in a tetragonal system gives unit-cell dimensions of 5.44898 Å by 12.65358 Å corresponding to a c/a ratio of 2.322 expected for an oxygen concentration of 1/6 indicating a hole doping of 1/3.

The NMR parameters were measured with home-built NMR equipment using standard pulse sequences by frequency sweeps at constant field. ^{61}Ni has $I=3/2$, and the standard diamagnetic NMR reference frequency based on $\text{Ni}(\text{CO})_4$ in our nominal 14 T magnetic field is $^{61}\omega/2\pi=53.5975$ MHz (a discussion of the location of reference frequencies in general is given in Ref. 15, in the following referred to as PNMRs). The high static field not only improves sensitivity but also separates the ^{61}Ni quadrupole satellites from those of ^{139}La .⁸ Most line positions in this paper are given in terms of K ,

$$K = (\omega/^{61}\omega) - 1. \quad (1)$$

$\text{La}_2\text{NiO}_{4+\delta}$. Figure 1(a) gives the results of a frequency sweep for $B||ab$ between 48 and 66 MHz at 230 K revealing the Ni quadrupole splitting,

$$\Delta_Q = \omega_Q(3 \cos^2 \theta - 1) \quad (2)$$

between the satellite transitions, with $\omega_Q/2\pi=11.3$ MHz. Here it has been supposed that the electric field gradient is symmetrical around the c axis so that in Fig. 1(a) $\theta=\pi/2$. In that case, the central transition should be shifted up in frequency by 0.45 MHz with respect to the center of the two satellites. For the field parallel to the c axis, the satellites have not been observed but should be spaced twice as large, and the central transition should be unshifted by quadrupolar effects. It follows that the difference in line positions of about 1 MHz in Figs. 1(b) and 1(c) can only partly be due to quadrupolar effects and a difference in Knight shifts plays a role as well.

A remarkable effect is a temperature hysteresis in the observability of these NMR signals. If the sample is cooled down rapidly (in an hour) from room temperature to ~ 200 K no signal is visible. By cooling down slowly to

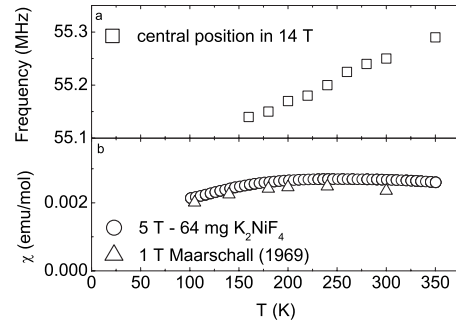


FIG. 2. (a) T dependence of the central transition of ^{61}Ni in a powder of K_2NiF_4 in a field of 14 T (proton frequency of 599.790 MHz) in the paramagnetic phase. (b) Susceptibility versus T of the same sample (circles) and results from Ref. 18.

225 K, then waiting for some hours followed by further cooling to 200 K (or by slowly heating to 270 K) the otherwise undetectable signals at these temperatures can be recorded. Comparable effects have been seen in the neutron data,¹² and by ^{139}La NMR in similar crystals as studied here.⁷ In the ^{139}La NMR experiment, above 230 K the ^{139}La nuclear relaxation is found to be primarily due to thermally activated charge fluctuations with an activation energy of 3×10^3 K, and hence the corresponding correlation rate for charge/oxygen motion strongly depends on T around 230 K.⁷ By cooling faster than the correlation rate, the oxygen will be frozen in random positions and the resulting distribution in quadrupolar couplings will wash out the spectrum. Slow cooling will allow the oxygen to get well arranged. The hysteresis occurs because the ordered dopants at low temperatures will keep their arrangement over some T range above the oxygen ordering temperature.¹² In contrast in $\text{La}_{5/3}\text{Sr}_{1/3}\text{NiO}_4$, which has a similar doping level but no excess oxygen and hence only mobile holes, the transition to charge order is of second order.^{9,16,17}

The intensity of the resonance lines in Figs. 1(b) and 1(c), normalized to the 250 K value, starts to decline severely below 110 K—a phenomenon that has been observed previously also by ^{139}La NMR.⁷

K_2NiF_4 . This compound is considered as the prototype of a 2D Heisenberg antiferromagnet.^{18,19} We followed the ^{61}Ni signal (natural abundance, powder sample) in the paramagnetic phase as a function of T . The central transition was detected by Fourier transform of half a spin echo, and had about 25 kHz full width at half maximum (the point-charge lattice electric field gradient is less than in the La nickelate because the K- and F-point charges are smaller than the La, respectively, O). The shift in K_2NiF_4 is T dependent, see Fig. 2(a), and more paramagnetic (the resonance occurs at higher frequencies or lower fields) with respect to the reference. The clearly T -dependent shift does not follow χ obtained from the magnetization measured in 5 T with a superconducting quantum interference device in the same T regime on the same powder as used in the NMR measurements. The measured χ closely resembles the 1 T data of Maarschall *et al.*,¹⁸ see Fig. 2(b). The spin-lattice relaxation time is less than a millisecond, as expected when magnetic fluctuations are important.

K_2NiF_6 . The measured ^{61}Ni shift in an unenriched powder of the Van Vleck paramagnet K_2NiF_6 $K=1.08 \times 10^{-2}$ is almost T independent. In this compound, Ni^{4+} has a cubic environment and hence no static quadrupole interaction; the spin-lattice relaxation times are long (on the order of 2 s at 200 K), as expected when no fluctuating-spin interactions are present.

III. ANALYSIS

The NMR shift of the nuclei of paramagnetic ions in dense paramagnets has been studied much less than that in Pauli-paramagnetic metals (for a review of the latter, see PNMRs). An important method of analysis of metal NMR is the Clogston-Jaccarino plot that correlates the spin contributions to the susceptibility and Knight shift (χ_S , respectively, K_S) with T as implicit parameter and gives the nuclear hyperfine field.²⁰ The relation follows from the nuclear-spin Hamiltonian (given in SI units and simplified for isotropic interactions),

$$\begin{aligned} \mathcal{H}_n &= -\hbar \gamma_{\text{ref}} (1 + \delta) \vec{B} \cdot \vec{I} + \hbar A \vec{I} \cdot \langle \vec{S} \rangle \\ &= -\hbar \gamma_{\text{ref}} \left[1 + \delta + \chi_S \frac{A}{g \gamma_{\text{ref}} \mu_B \mu_0} \right] \vec{B} \cdot \vec{I} \end{aligned} \quad (3)$$

with Ω the volume of the simple unit cell and δ the chemical shift. The last term in the parentheses denotes the Knight shift K_S . Traditionally susceptibilities are given in the cgs unit of emu/mole, leading to

$$K_S = (\chi_{\text{mol}}/N_A \mu_B) (A/\gamma_{\text{ref}} g) \quad (4)$$

with χ_{mol} the molar susceptibility, N_A Avogadro's number, μ_B the Bohr magneton (in cgs units), and g the Landé g factor. The combination $A/(\gamma_{\text{ref}} g)$ is referred to as the hyperfine field per Bohr magneton, and A/γ_{ref} as the hyperfine field per unit electronic spin—both in Oe/G. Usually A is independent of T so that the Clogston-Jaccarino plot of K_S versus χ_S yields a straight line, where the slope is a direct measure of the hyperfine field.

The K_S - χ relation for the planar Cu(2) sites in $\text{YBa}_2\text{Cu}_3\text{O}_x$ has been analyzed by this method,^{21–23} where in Ref. 23 the relevant parameters are evaluated in the context of a crystal-field model (see also the Appendix). Again χ and the shift can be split into a T -independent orbital and a T -dependent spin part. Due to the almost tetragonal symmetry of the unit cell, the hyperfine interaction in Eq. (4) is anisotropic and often an extra term $\sum_{j=1}^4 B_j \vec{S}_j$ is added to take the transferred interaction into account.^{21,22} In underdoped $\text{YBa}_2\text{Cu}_3\text{O}_{6.63}$, K in the c direction does not vary with T . It means that the on-site (T -dependent) spin part and supertransferred hyperfine fields cancel each other: $A_{\parallel} + 4B \approx 0$.²⁴

Quite some NMR properties of paramagnetic ions in dilute diamagnetic hosts have been derived from electron-nuclear double resonance (ENDOR) [and electron spin resonance (ESR)] experiments. Two kind of results are especially relevant: often a so-called pseudonuclear Zeeman effect is found, which is the equivalent of the T -independent chemical shift in diamagnetic molecules or of the Van Vleck contribu-

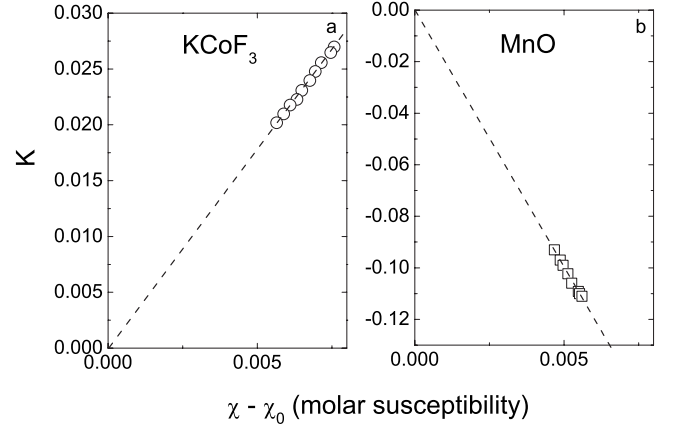


FIG. 3. Clogston-Jaccarino plots for (a) KCoF_3 based on the data quoted in the text and (b) MnO based on data published in Ref. 33.

tion to the Knight shift in metals;²⁵ furthermore supertransferred hyperfine interactions are found on diamagnetic ions of the matrix (such as Al^{3+}) that are separated from the dilute paramagnetic ion (such as Fe^{3+}) by a ligand (such as O).²⁶ A detailed ENDOR experiment on Ni^{2+} in (trigonal) Al_2O_3 yields a T -independent shift of 0.028 and a net ^{61}Ni hyperfine field of ~ -9 T per unit spin.²⁷ For Co^{2+} in MgO , there is a huge T -independent shift of 0.39 ± 0.01 ,²⁸ and a hyperfine field per unit spin of 29 T. In the Appendix, which gives some details on the relation between NMR and ENDOR/ESR parameters, we argue that in MgO , a hypothetical NMR experiment would see clearly distinct signals for $^{61}\text{Ni}^{2+}$ and $^{61}\text{Ni}^{3+}$.

A. Metal-ion NMR in the paramagnetic phase of antiferromagnets

We are interested in antiferromagnetic systems for which both ingredients for the Clogston-Jaccarino plot are available from experiments. From the literature, these data can be found for the 3D magnets MnO (cubic) and KCoF_3 (perovskite); here we will add new data on the 2D magnet K_2NiF_4 .

KCoF_3 . The Clogston-Jaccarino plot for KCoF_3 ($T_N=114$ K) given in Fig. 3(a) has not been published before but the χ data are available from Ref. 29 and the NMR data from Ref. 30. We have plotted the shifts with respect to a reference $\gamma/2\pi=10.03$ MHz/T expected from suitably corrected values found in ionic solutions of Co^{3+} (see PNMRs); from the χ data the T -independent background χ_0 has been subtracted. The rather amazing result is that the T -independent shift of 0.39 from the ENDOR data is absent,^{28,30} although it has also been seen in the ordered low- T phase.^{31,32} A single data point for paramagnetic CoO likewise fails to show this large shift.³⁰ The slope in Fig. 3 gives a hyperfine field per Bohr magneton of 20 T. Although the analysis of the ^{59}Co hyperfine field is very complex,²⁸ it does not suggest that Co-Co transferred hyperfine fields are important.

MnO . Also in the paramagnetic phase of MnO ($T_N=117$ K) transferred hyperfine fields have no noticeable

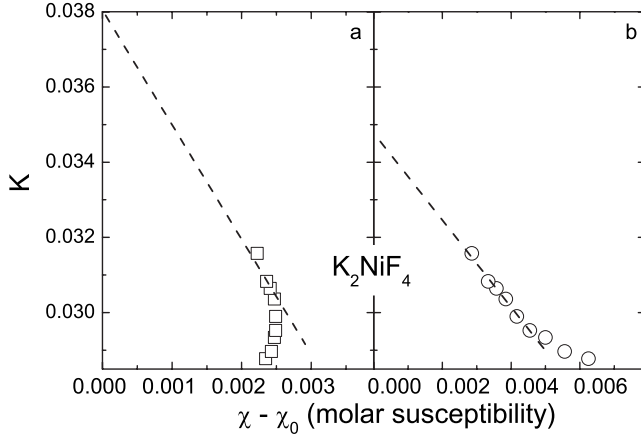


FIG. 4. Clogston-Jaccarino plots for K_2NiF_4 . (a) K is plotted versus the experimental susceptibility. (b) K versus χ of a free Ni^{2+} ion with $g=2.28$. For a discussion of the dashed lines, see text.

influence, see Fig. 3(b) based on ^{55}Mn NMR (after Ref. 33). The extrapolation shows no T -independent shifts, which is indeed expected for Mn^{2+} on theoretical grounds, see Abragam and Bleaney (referred to as AB70).³⁴ The slope yields a hyperfine field per Bohr magneton of -11.5 T, or, using $g \sim 2$, of -23 T per unit spin, which goes very well with data reviewed in AB70 for Mn^{2+} diluted in simple cubic oxides but does not support the theoretical expectation that in MnO , the hyperfine should increase (in absolute value) by approximately 4.2 T with respect to the value in dilute systems.³⁵ For our later discussion, it is important to remember that this theoretically expected change is anyway relatively small.

K_2NiF_4 . This compound ($T_N=100.5$ K) is the paradigm of an $S=1$ Heisenberg square-planar antiferromagnet and the remarkable behavior of χ in Fig. 2(b) in the paramagnetic phase is theoretically well understood.¹⁹ It is related to the buildup of correlations $\langle S_{z,i} S_{z,j} \rangle$ between neighboring $(i,j)\text{Ni}^{2+}$ spins. Experimentally, the existence of such correlations has been derived by Maarschall *et al.* from T_2 (actually linewidth) measurements on ^{19}F .¹⁸ It is immediately clear from Fig. 2 that no straight-line correlation exists between shift and susceptibility: in the experimentally accessible T range, the hyperfine field and χ have different T dependencies. As discussed in the Appendix, we think this to be due to a different influence of *static* effects of the correlations $\langle S_{z,i} S_{z,j} \rangle$ on the transferred hyperfine field and on χ , not seen in the experimentally accessible T regions for cuprates. This interesting effect has no consequences for the estimate of the hyperfine field, which is also needed for the analysis of La_2NiO_4 .

We want to estimate the hyperfine field in the regime where χ is Curie-Weiss type. From the theoretical fits in Ref. 19, such behavior is expected to occur at higher temperatures ($T > 500$ K) than we could attain in Fig. 2. For $T > 500$ K, the Clogston-Jaccarino plot should become a straight line and for $T^{-1} \rightarrow 0$, we should find the T -independent shift. Two attempts at such a fit are shown in Fig. 4. The χ axis in Fig. 4(a) uses the experimental data from Fig. 2(b) ($\chi_0=0$), and in Fig. 4(b) the theoretical value for the Curie susceptibility of

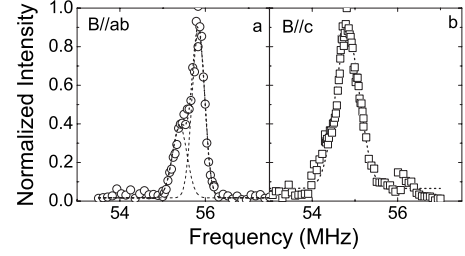


FIG. 5. Decomposition of the ^{61}Ni line in $\text{La}_2\text{NiO}_{4.17}$ for (a) $B \parallel ab$ and (b) $B \parallel c$ at 130 K. Dashed lines are Gaussian fits (see text); in (a) the two lines have an intensity ratio of 1:2.

independent spins (again $\chi_0=0$) with $S=1$ and $g=2.28$ (see also the Appendix) as found for dilute Ni^{2+} in the perovskite KMgF_3 .³⁶ The extrapolated values for the line position are, somewhat arbitrarily, taken as 55.635 MHz in Fig. 2(a) and 55.474 MHz in Fig. 2(b) corresponding to T -independent contributions to the Knight shift of 3.8×10^{-2} and 3.5×10^{-2} , roughly three times the value in the Van Vleck compound K_2NiF_6 . The first observation is that the slopes of both straight lines indicate a negative hyperfine field associated with the Curie contribution; the second that the absolute value of this field [1.5 T in a and 0.7 T in b, expressed per Bohr magneton] is much smaller than the 4 T found in the ENDOR experiment.^{25,27} A hyperfine field of 4 T would yield a much steeper slope, and extrapolate to unlikely values for the T -independent shift. The relatively small slopes indicate that in the paramagnetic phase of a simple 2D antiferromagnet the sum of the on-site hyperfine field and the transferred hyperfine fields can be very small indeed. This cancellation is similar to what is found in the cuprates but very different from the available results for the 3D antiferromagnets in Fig. 3.

B. Doped La_2NiO_4

The ^{61}Ni NMR spectrum for the field $\vec{B} \parallel ab$, see Fig. 1(b), has a double-peaked structure at 250 K, that becomes a shoulder at 90 K. The line shape at 130 K is shown in Fig. 5(a), together with a fitted decomposition into two Gaussian lines. Apart from the shiny crystal surfaces and the sharpness of the x-ray diffraction pattern (not shown), the structure has to be intrinsic and not due to different crystal domains or accidental inhomogeneities in the static distribution of dopant oxygen for the following reasons: (i) unenriched $\text{La}_2\text{NiO}_{4.17}$ crystals measured previously show a similar splitting below 250 K for the ^{139}La NMR transition between the $-3/2$ and $-1/2$ levels and not in the $-1/2-1/2$ transition, which is a proof of its quadrupolar origin.⁷ (ii) The line shapes are very reproducible from one T run to another. Since each run starts at high temperatures, where the oxygen diffuse rather freely, it is unlikely that different runs end up with similar inhomogeneities. In view of these arguments, we assign the two-peaked structure to doped and undoped plaquettes. The intensity ratio 0.35 ± 0.05 to 0.65 ± 0.05 in Fig. 5(a) is indeed as expected in this scenario.

The ^{61}Ni NMR data in Fig. 2(a) are the only ones available for what is undoubtedly Ni^{2+} , and from the ESR data for

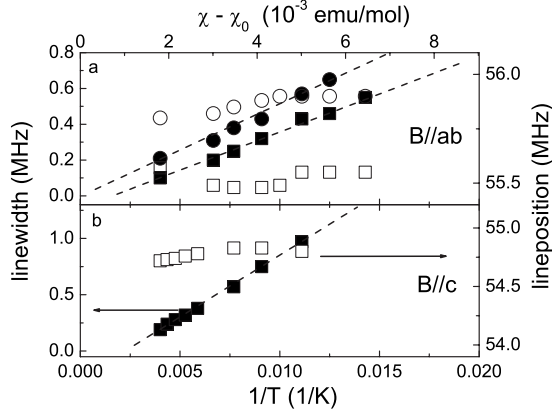


FIG. 6. Linewidth (full symbols—left axis) and position (open symbols—right axis) of the ^{61}Ni resonance in $\text{La}_2\text{NiO}_{4.17}$ for (a) $B\parallel ab$ and (b) $B\parallel c$ versus $1/T$ (bottom axis) and $\chi - \chi_0$ (top axis). The reference value for the ^{61}Ni line position in the applied field is 53.60 MHz. Dashed lines are fits discussed in the text.

Ni^{3+} discussed in the Appendix, the NMR shifts for $^{61}\text{Ni}^{3+}$ and $^{61}\text{Ni}^{2+}$ are expected to differ markedly. Hence the small line splitting in Fig. 5(a) is not due to a difference in hyperfine interaction but has to be ascribed to a difference in electric field gradients felt by the Ni ion, giving additional evidence for the location of the holes on the oxygen as deduced by Schüßler-Langenhene *et al.*⁶ This electric scenario is supported by the splitting of the ^{139}La $m=3/2$ resonance below the same temperature of 250 K (mentioned above), which was proven to be a quadrupolar effect.⁷ Also the broadening of the spectra with decreasing T has to be explained in terms of a redistribution of charges on the surrounding oxygen (see below). In most cuprates holes in the CuO_2 plane have a much higher mobility and such a decomposition cannot be made.

For $\vec{B}\parallel c$, see the discussion of Eq. (2), both quadrupolar and magnetic (Knight) effects can be different from the $\vec{B}\parallel ab$ case. The line shape in Fig. 5(b) shows only the slightest hint of a low-frequency shoulder, and for this orientation we simply fit the data to a single Gaussian. The clearly much larger width in Fig. 5(b) is nevertheless compatible with the idea that we still have two lines but the accuracy of a further resolution is too small to be meaningful.

Clogston-Jaccarino plots of both the line positions and widths against χ are shown in Fig. 6. The susceptibility on samples with well-known oxygen stoichiometries has been published by Odier *et al.*,³⁷ and for samples similar to ours by Bernal *et al.* and Abu-Shiekh *et al.*^{7,38} For $\text{La}_2\text{NiO}_{4.17}$, the χ data are in good agreement with each other, and can be described by a Curie-Weiss law with an almost T -independent background χ_0 .

The central positions at 54.75 MHz for $B\parallel c$ and 55.55/55.90 MHz for $B\perp c$ at 250 K are hardly T or χ dependent. The data thus imply that the Ni nuclei experience an almost complete cancellation of the direct hyperfine field by the transferred contribution, reminiscent to K_2NiF_4 . The shifts with respect to the reference value of 53.60 MHz can be due to second-order quadrupolar effects (see above) and/or Van Vleck shifts.

Below 250 K, the ^{61}Ni line grows in width with decreasing T but its intensity remains Curie type down to 110 K, where the signal starts to get wiped out due to magnetic fluctuations.^{7,8,39,40} In general, the line broadening can be due to a (re)distribution of local static magnetic fields or electric field gradients but here T is too high for a static magnetic scenario. It implies that the Ni ions experience an increasing spread in the static (on the NMR time scale) electrical field gradients, as expected when charge-density waves or striped structures develop. The charge modulation affects not only the Ni ions of the doped but also of the undoped plaquettes. Also in unenriched $\text{La}_2\text{NiO}_{4.17}$ crystals using ^{139}La NMR quadrupolar effects are seen to dominate above 140 K.⁷ In $\text{La}_{5/3}\text{Sr}_{1/3}\text{NiO}_4$ below the charge order temperature of 240 K, a redistribution of holes has been observed too.^{9,16,17}

IV. CONCLUSIONS

In the literature on ^{63}Cu NMR in the 2D cuprates, it has been accepted as an experimental fact that direct and supertransferred hyperfine fields can cancel each other. We have pointed out that for such a cancellation in 3D systems, the available data show no indication. On the other hand, the extrapolation of our data for K_2NiF_4 in Fig. 4, and those in Fig. 6 for $\text{La}_2\text{NiO}_{4.17}$, both 2D antiferromagnets, suggest that this cancellation might be a more frequent phenomenon for 2D systems.

In paramagnetic K_2NiF_4 not too far above T_N , the Clogston-Jaccarino relation between susceptibility and Knight shift is not linear. This unique feature is explained by a difference in sensitivity for correlations of these two parameters, which probe different facets of the electronic spin.

Regarding the nickelates, the ^{61}Ni NMR line position is different for $B\parallel c$ and $B\perp c$, and doped and undoped NiO_4 plaquettes can be discriminated by their line shift found by decomposition of the resonance line for $B\perp c$. The analysis shows that the doped holes are located on the neighboring oxygen in agreement with the resonant soft x-ray diffraction of Schüßler-Langeheine *et al.*⁶ From the growing linewidth with decreasing temperature and the results of a previously made ^{139}La NMR study,⁷ we conclude that between 250 and 140 K, the holes experience a redistribution that changes the electrical field gradients at the Ni site—a process consistent with the formation of charge-density waves or (short) stripes.

ACKNOWLEDGMENTS

We thank Yakov Mukovskii and his co-workers of the Moscow State Steel and Alloys Institute for the synthesis and growing of the enriched single crystals and Ruud Hendrikx of the Technical University of Delft for the crystal diffraction analysis. The powder of K_2NiF_4 was kindly provided by Dany Carlier (ICMCB-CNRS, Bordeaux). Stimulating discussions with Jan Zaanen are highly appreciated.

APPENDIX: K AND χ OF Ni^{2+}

Dilute paramagnets. For experimental reasons, hardly any NMR exists on dilute transition-metal ions in a diamagnetic

host but hyperfine fields can still be found from ENDOR data. A didactic treatment of this procedure, using Ni^{2+} as example, has been given by Geschwind.²⁵ The ground term of the free $3d^8$ ion has $L=3$ and $S=1$. The sevenfold orbital degeneracy of the free ion is lifted by the cubic crystal field into a low-lying orbital singlet and two excited orbital triplets. Perturbation theory of the magnetic-resonance properties of Ni^{2+} considers only these three sets of states. In first order, when only the orbital singlet is considered, the orbital moment is quenched: the electronic $g=2$, there is only a Curie susceptibility $\propto 1/T$, and the NMR shift is determined by this susceptibility and the core-polarization hyperfine field. In second order, new contributions appear: the electronic g shift Δg (a cross term between the spin-orbit Hamiltonian and the orbital part of the electron Zeeman Hamiltonian), the orbital hyperfine field (a cross term between the spin-orbit and the orbital hyperfine Hamiltonians), the paramagnetic shielding of the nuclear Zeeman coupling (a cross term between the orbital hyperfine Hamiltonian and the orbital part of the electron Zeeman Hamiltonian) and the T -independent contribution to χ (a cross term of the orbital part of the Zeeman Hamiltonian with itself). Apart from a multiplicative constant, the paramagnetic shielding can also be written as a product of the T -independent susceptibility and the orbital hyperfine field. At this level of perturbation, there is no dipolar part in the hyperfine Hamiltonian (but it appears in lower symmetry).

The Hamiltonian for the effective electron spin S , \mathcal{H}_S , can be written as

$$\mathcal{H}_S/\hbar = \beta \vec{B} \cdot (2 + \vec{\Delta}g) \cdot \vec{S} + \vec{S} \cdot \vec{A} \cdot \vec{I} - \gamma_I(1 + \delta)\vec{B} \cdot \vec{I}, \quad (\text{A1})$$

where we have omitted an additional term for the zero-field splitting, which is unimportant for our purpose,²⁷ and the nuclear quadrupole coupling. The effective hyperfine tensor \vec{A} now contains both the (negative) core-polarization and (positive) orbital hyperfine fields and is to a good approximation an “ionic” property, independent of the host. The paramagnetic shielding is represented by δ . The Knight shift Hamiltonian that corresponds to Eq. (A1) is

$$\mathcal{H}_I/\hbar = \langle \vec{S} \rangle \cdot \vec{A} \cdot \vec{I} - \gamma_I(1 + \delta)\vec{B} \cdot \vec{I}, \quad (\text{A2})$$

of which Eq. (4) is a simplified form. In that equation, the value of Δg shows up explicitly in the expression for χ_S .

The low-spin $^{61}\text{Ni}^{3+}$ has been seen in MgO by ESR, together with $^{61}\text{Ni}^{2+}$.^{41,42} The paramagnetic shielding has not been determined. For Ni^{3+} , the g shift is 0.17 and the absolute value of the hyperfine field 6.71 T; for Ni^{2+} the values are 0.22 and 6.45 T. In general, the crystal-field analysis for the $3d^7$ configuration is rather complicated (the typical case is Co^{2+} , $S=3/2$) (Ref. 28) but for the low-spin configuration strong ligand field theory applies. There is just a single electron in the $d\gamma$ shell, which makes the magnetic-resonance behavior very similar to that of $3d^9\text{Cu}^{2+}$ with a single hole in the $d\gamma$ shell.³⁴ Even though the paramagnetic shielding of $^{61}\text{Ni}^{3+}$ is not known, one may assume that in a hypothetical

NMR experiment on these dilute impurities in MgO, two clearly distinct signals would be observed for the two Ni valencies.

Dense paramagnets. A typical extension of crystal-field theory to the NMR of the “magnetic” nuclei in dense paramagnets is provided by the discussion of $^{63}\text{Cu}^{2+}$ in the $\text{YBa}_2\text{Cu}_3\text{O}_x$ system.²³ The main new contribution that appears is the supertransferred hyperfine field, due to the presence of the neighboring magnetic ions. Schematically it can be thought of as due to a very small $4s$ admixture created by the super exchange; s electrons have a large positive direct hyperfine field, so even a small admixture can cause measurable effects.

In dense paramagnetic systems such as KCoF_3 and CoO ,³⁰ it is found experimentally (see Fig. 3) that the paramagnetic shielding is much smaller than in dilute paramagnets. This is likely related to an exchange narrowing of both spin and orbital interactions³⁰ but in Eq. (A2), the $\langle \vec{S} \rangle$ part remains proportional to χ_S and δ remains T independent in the relevant T range. Further support for this hypothesis comes from the experimental data in the low- T antiferromagnetic phase,^{31,32} where the exchange becomes static and essentially the same δ as in the dilute systems is found.

For the Ni^{2+} ion, the g value remains close to 2 even with an additional trigonal distortion, as in the case of an Al_2O_3 host, where ENDOR measurements have been made.²⁷ These data yield a “pseudonuclear Zeeman” shift of 0.028, which is comparable to the Van Vleck shift of ≈ 0.011 that we have measured in $S=0$ K_2NiF_6 . The T -independent shift in K_2NiF_4 (the extrapolations in Fig. 4) can be expected to have a comparably small value; all the more so because this is a dense paramagnet and exchange narrowing (see above) might be operative.³⁰

We made the choice of $g=2.28$ and $S=1$, taken from data on KMgF_3 , to plot the dashed line in Fig. 4(b). The choice of g value is somewhat arbitrary—we preferred a fluoride host for the comparison. The values in Al_2O_3 , MgO , and CaO range from 2.18 to 2.33; any of these would not change our main conclusion that a reasonable estimate for the hyperfine field would come out at a much smaller value than in the dilute systems. The spin value should be $S=1$, both in oxides and in fluorides.

The difference between the negative slope in Fig. 3(b) and the positive slope in Fig. 3(a) comes from the Δg effect: dilute Mn^{2+} has very nearly $\Delta g=0$, see AB70, and therefore an almost pure core-polarization hyperfine field.

The difference between susceptibility and shift. When the effects of correlations are included in χ , see Ref. 19 for the original references, χ has to be written as

$$\chi = \frac{C}{T} \sum_{i=0}^{\infty} \frac{3\langle S_{z,0}S_{z,i} \rangle}{S(S+1)}, \quad (\text{A3})$$

where i runs over all spins. If there are only on-site (or auto) correlations (a simple paramagnet) $\langle S_{z,0}S_{z,i} \rangle = \frac{1}{3}S(S+1)$ and one retrieves the Curie law.

To understand that the correlations also have an effect on the transferred hyperfine fields it is instructive to compare

the reasoning usually applied to the cuprates with that for an ordered antiferromagnetic phase.^{25,35,43} In the cuprates, correlations are neglected and therefore the transferred field has the opposite sign to the on-site core-polarization field. In the

fully correlated phase, the transferred field has the same sign. Therefore, when correlations start to grow in the paramagnetic phase, the total hyperfine field becomes more negative, similar to what is seen in Fig. 4(a).

- ¹F. C. Zhang and T. M. Rice, Phys. Rev. B **37**, 3759 (1988).
- ²J. Zaanen and O. Gunnarsson, Phys. Rev. B **40**, 7391 (1989).
- ³For a review and references, see, e.g., H. B. Brom and J. Zaanen, in *Handbook of Magnetic Materials*, edited by J. Buschow (Elsevier, Amsterdam, 2003), Vol. 15, Chap. 4.
- ⁴J. M. Tranquada, B. J. Sternlieb, J. D. Axe, Y. Nakamura, and S. Uchida, Nature (London) **375**, 561 (1995).
- ⁵J. Zaanen and P. B. Littlewood, Phys. Rev. B **50**, 7222 (1994); E. Pellegrin, J. Zaanen, H.-J. Lin, G. Meigs, C. T. Chen, G. H. Ho, H. Eisaki, and S. Uchida, *ibid.* **53**, 10667 (1996).
- ⁶C. Schüßler-Langeheine, J. Schlappa, A. Tanaka, Z. Hu, C. F. Chang, E. Schierle, M. Benomar, H. Ott, E. Weschke, G. Kaindl, O. Friedt, G. A. Sawatzky, H.-J. Lin, C. T. Chen, M. Braden, and L. H. Tjeng, Phys. Rev. Lett. **95**, 156402 (2005).
- ⁷I. M. Abu-Shiekh, O. O. Bernal, A. A. Menovsky, H. B. Brom, and J. Zaanen, Phys. Rev. Lett. **83**, 3309 (1999); I. M. Abu-Shiekh, O. O. Bernal, H. B. Brom, M. L. de Kok, A. A. Menovsky, J. T. Witteveen, and J. Zaanen, arXiv:cond-mat/9805124 (unpublished).
- ⁸I. M. Abu-Shiekh, O. Bakharev, H. B. Brom, and J. Zaanen, Phys. Rev. Lett. **87**, 237201 (2001).
- ⁹C.-H. Du, M. E. Ghazi, Y. Su, I. Pape, P. D. Hatton, S. D. Brown, W. G. Stirling, M. J. Cooper, and S.-W. Cheong, Phys. Rev. Lett. **84**, 3911 (2000).
- ¹⁰D. E. Rice and D. J. Buttrey, J. Solid State Chem. **105**, 197 (1993).
- ¹¹S. Hosoya, T. Omata, K. Nakajima, K. Yamada, and Y. Endoh, Physica C **202**, 188 (1992).
- ¹²J. M. Tranquada, D. J. Buttrey, V. Sachan, and J. E. Lorenzo, Phys. Rev. Lett. **73**, 1003 (1994).
- ¹³A. Mehta and P. J. Heaney, Phys. Rev. B **49**, 563 (1994).
- ¹⁴H. Tamura, A. Hayashi, and Y. Ueda, Physica C **258**, 61 (1996).
- ¹⁵J. J. van der Klink and H. B. Brom, Prog. Nucl. Magn. Reson. Spectrosc. **36**, 89 (2000), referred to as PNMRS.
- ¹⁶S.-H. Lee and S.-W. Cheong, Phys. Rev. Lett. **79**, 2514 (1997).
- ¹⁷S.-H. Lee, S.-W. Cheong, K. Yamada, and C. F. Majkrzak, Phys. Rev. B **63**, 060405(R) (2001).
- ¹⁸E. P. Maarschall, A. C. Botterman, S. Vega, and A. R. Miedema, Physica **41**, 473 (1969).
- ¹⁹L. J. de Jongh and A. R. Miedema, Adv. Phys. **50**, 947 (2001); reprint from **23**, 1 (1974).
- ²⁰A. M. Clogston and V. Jaccarino, Phys. Rev. **121**, 1357 (1961); A. M. Clogston, V. Jaccarino, and Y. Yafet, *ibid.* **134**, A650 (1964).
- ²¹M. Takigawa, A. P. Reyes, P. C. Hammel, J. D. Thompson, R. H. Heffner, Z. Fisk, and K. C. Ott, Phys. Rev. B **43**, 247 (1991).
- ²²H. Monien, D. Pines, and M. Takigawa, Phys. Rev. B **43**, 258 (1991).
- ²³T. Shimizu, H. Aoki, H. Yasuoka, T. Tsuda, Y. Ueda, K. Yoshimura, and K. Kosuge, J. Phys. Soc. Jpn. **62**, 3710 (1993).
- ²⁴In $\text{Ti}_2\text{Ba}_2\text{CuO}_6$, the values of the Cu hyperfine coupling constant differ from those in 123 or 214 compounds, presumably due to the 6s orbital of the Ti ion and the location of the apical oxygen, see, e.g., H. B. Brom, D. Reefman, J. C. Jol, D. M. de Leeuw, and W. A. Groen, Phys. Rev. B **41**, 7261(R) (1990).
- ²⁵S. Geschwind, in *Hyperfine Interactions*, edited by A. J. Freeman and R. B. Frankel (Academic Press, New York, 1967).
- ²⁶D. R. Taylor, J. Owen, and B. M. Wanklyn, J. Phys. C **6**, 2592 (1973).
- ²⁷P. R. Locher and S. Geschwind, Phys. Rev. Lett. **11**, 333 (1963).
- ²⁸D. J. I. Fry, P. M. Llewellyn, and M. H. L. Pryce, Proc. R. Soc. London, Ser. A **266**, 84 (1962).
- ²⁹K. Hirakawa, J. Phys. Soc. Jpn. **19**, 1678 (1964).
- ³⁰R. G. Shulman, Phys. Rev. Lett. **2**, 459 (1959).
- ³¹V. Jaccarino, Phys. Rev. Lett. **2**, 163 (1959).
- ³²T. Moriya, J. Phys. Chem. Solids **11**, 175 (1959).
- ³³E. D. Jones, Phys. Rev. **151**, 315 (1966).
- ³⁴A. Abragam and B. Bleaney, *Electron Paramagnetic Resonance* (Clarendon Press, Oxford, 1970).
- ³⁵N. L. Huang, R. Orbach, E. Šimánek, J. Owen, and D. R. Taylor, Phys. Rev. **156**, 383 (1967).
- ³⁶W. M. Walsh (private communication); as quoted in R. G. Shulman and S. Sugano, Phys. Rev. **130**, 506 (1963).
- ³⁷P. Odier, N. J. Poirrot, P. Simon, and D. Desousa Meneses, Eur. Phys. J.: Appl. Phys. **5**, 123 (1999).
- ³⁸O. O. Bernal, H. B. Brom, M. L. de Kok, J. Witteveen, and A. A. Menovsky, Physica C **282-287**, 1393 (1997).
- ³⁹G. B. Teitelbaum, I. M. Abu-Shiekh, O. Bakharev, H. B. Brom, and J. Zaanen, Phys. Rev. B **63**, 020507(R) (2000).
- ⁴⁰A. W. Hunt, P. M. Singer, A. F. Cederström, and T. Imai, Phys. Rev. B **64**, 134525 (2001).
- ⁴¹J. W. Orton, J. E. Wertz, and P. Auzins, Phys. Lett. **6**, 339 (1963).
- ⁴²U. Höchli, K. A. Müller, and P. Wysling, Phys. Lett. **15**, 5 (1965).
- ⁴³F. Mila and T. M. Rice, Physica C **157**, 561 (1989).